Quasi 10-day wave modulation of equatorial ionization anomaly during the Southern Hemisphere stratospheric warming of 2002

Xiaohua Mo[1]，Donghe Zhang[2*]

[1]College of Science, Key Laboratory for Ionospheric Observation and Simulation, Guangxi University for Nationalities, Nanning, China

[2]Department of Geophysics, Peking University, Beijing, 100871, China

Correspondence: Donghe Zhang (zhangdh@pku.edu.cn)

Abstract

The present paper studies the perturbations in equatorial ionization anomaly (EIA) region during the Southern Hemisphere (SH) sudden stratospheric warming (SSW) of 2002, using the location of EIA crests derived from Global Positioning System (GPS) station observations，the Total Electron Content (TEC) obtained by International GNSS Service (IGS) global ionospheric TEC map (GIMs), and the equatorial electrojet (EEJ) estimated by geomagnetic field in Asian sector. The results indicate the existence of an obvious quasi 10-day periodic oscillation in the location and TEC of northern and southern EIA crest. An eastward phase progression of quasi 10-day wave producing the SH SSW of 2002 is also identified in polar stratospheric temperature. Previous studies have shown that a strong quasi 10-day planetary wave with zonal wave numbers s=1 extend from the lower stratosphere to mesosphere and lower thermosphere during the SH SSW of 2002 (Palo et al., 2005). Moreover, the EEJ driven by equatorial zonal electric field exhibits quasi 10-day oscillation, suggesting the enhanced quasi-10-day planetary wave associated with SSW penetrates into the ionosphere E region and produces oscillation in EIA region through modulating the E-region electric fields. Our results reveal some newer features of ionospheric variation that have not been reported during Northern Hemisphere (NH) SSWs.

1. Introduction

Sudden stratospheric warming (SSW) is large-scale meteorological process in the polar stratosphere which is characterized by rapid rise in temperatures and deceleration/reversal in the zonal mean flows (Scherhag, 1952). The primary driver of SSW is thought to be a rapid growth of quasi-stationary planetary wave interacting with zonal mean flow (Matsuno, 1971). Although the main processes of SSW occur in the polar middle atmosphere, its effects on the ionosphere have been observed in significant changes of equatorial electrojet (EEJ), vertical plasma drift, and equatorial ionization anomaly (EIA) (Vineeth et al., 2007; Chau et al., 2009; Goncharenko et al., 2010; Pancheva and Mukhtarov, 2011; Jin et al., 2012).

Since stationary planetary waves in the Southern Hemisphere (SH) generally have smaller amplitudes than in the Northern Hemisphere (NH) where orographic and thermal forcing is stronger (Andrews et al., 1987), major SSWs often occur in NH. Therefore, most studies about SSW effects on the ionosphere are during NH SSW period. In recent years, a great deal of research has been focused on the variation of the low latitude ionosphere during SSW period in the northern hemisphere, and the quasi-16-day periodic disturbance and the lunar tide characteristics have been found in some ionospheric parameters, for example, EEJ, vertical plasma drifts, ionospheric electron density (Vineeth et al., 2007; Chau et al., 2009; Pedatella and Forbes, 2009; Goncharenko et al., 2010). Some researchers considered that this kind of quasi-16-day periodic variations is related to the enhanced planetary wave during the SSW period (Chau et al., 2009; Pedatella and Forbes, 2009; Liu et al., 2010). But others believe that this kind of quasi-16-day period is related to the semi-diurnal lunar tides (Fejer et al., 2010; Park et al., 2012). The direct evidence is the typical SSW feature appears in some ionospheric parameters as morning enhancement and afternoon decrease, in a semi-diurnal pattern that progresses to later local times within several days. However, some studies believe that the local time variation characteristics are not necessarily caused by the semidiurnal lunar tides, Pedatella et al. (2012) demonstrate that the phase of the semidiurnal solar tide changes in a manner that makes it similar to the phase of the lunar semidiurnal tide. Besides, although many studies on the variation of the low latitude ionosphere during the SSW period, the physical connection between the SSW in the polar region and the featured variations in low latitude ionosphere is still not clear. Some studies even consider that the SSW and the featured variation of low latitude ionosphere is co-source, which is the effect of enhanced planetary waves in different regions (Stening et al., 2011).

In comparison, the atmospheric parameters in the mesosphere and lower thermosphere (MLT) are very limited. The atmospheric variation in MLT is usually indirectly reflected through the EEJ obtained from the

geomagnetiic field data in equatorial and low latitude region. The EEJ is driven by zonal electric field which also produces EIA via upward E×B drift (fountain effect). The zonal electric field modulated by tidal winds in the lower thermosphere through the E-region dynamo process is easy to be influenced by various atmospheric waves, so these ionospheric variations often display similar semidiurnal pattern and 13- to 16-day wave signatures which have been associated with enhanced planetary wave, solar and lunar tide wave during SSW period (Pedatella and Forbes, 2009; Goncharenko et al., 2010; Fejer et al., 2010;Park et al., 2012).

In August to September 2002, three minor SSWs and a major SSW appeared in SH (Varotsos 2002; Baldwin et al., 2003). There is sufficient evidence that a series of unusual atmospheric states occurred in this period, i.e., planetary wave scale quasi 10-day variation (Krüger et al., 2005; Palo et al., 2005), short-term semidiurnal tide variability with zonal wave number s=1 (Chang et al., 2009) and the winds oscillation with ~14-days period (Andrew et al., 2004), are all linked to the extremely large planetary wave events. Although the atmospheric activity in connection with 2002 SH SSW has been well revealed in observations and numerical modeling, relatively little is known about the ionosphere effects of 2002 SH SSW. Recently, Olson et al. (2013) studied the equatorial electrodynamic perturbations in Peruvian sector during 2002 SH SSW and found enhanced quasi 2-day fluctuations and large amplitude multi-day perturbations in EEJ and vertical drifts. The research of ionospheric behavior during SH SSW periods are useful for verifying the existing explanation about the origin of ionospheric perturbations during NH SSW periods and revealing some newer features of ionospheric variation, so further investigation of 2002 SH SSW effect on ionosphere with more ionospheric parameters is still warranted.

In the present study, we present the first observational evidence of quasi 10-day oscillation in EIA region during 2002 SH SSW which has not been reported during NH SSWs, based on the location of EIA crests derived from Global Positioning System (GPS) station observations, the Total Electron Content (TEC) obtained by International GNSS Service (IGS) global ionospheric TEC map (GIMs), and the EEJ estimated by geomagnetic field in Asian sector.

2. Data and Methods

The location of EIA crests derived from GPS observations are used to analyze the variation in EIA region during 2002 SH SSW from July 20, 2002 to October 27, 2002. The GPS stations are GUAN (23.19°N, 113.34°E, MLAT~12.52°N) and BAKO (6.49°S, 106.84°E, MLAT~17.18°S) which are near

northern and southern EIA crest, respectively. The locations of the GPS stations are shown in Figures 1. Since the ionospheric vertical TEC usually reach the maximum at EIA crest, the location of EIA crest can be obtained by vertical TEC values at each ionospheric penetration point (IPP), which is the intersection of the line of sight and the ionospheric shell (assumed to be 400 km) (Mo et al., 2014). The relative accuracy of the TEC is 0.02 total electron content unit (1TECU=10^{16} el m^{-2}) (Hofmann-Wellenhof et al., 1992). The sample rate of these GPS stations were 30s, so the resolution of the location of EIA crest is less than 25 km (Mo et al., 2017). Figures 2a and 2b show the daily average geomagnetic latitude (MLAT) of northern and southern EIA crests during 2002 SH SSW.

The TEC from GIMs are also used to analyze the variation in EIA region. The GIMs provides maps of TEC obtained from a global network of GPS receivers, which have temporal resolution of 2 hours and spatial resolution of 5° in longitude and 2.5° in latitude (Mannucci et al., 1998). The EIA crest usually reaches its maximum development near 14:00 LT (Huang et al., 1989; Yeh et al., 2001), so the daily average TEC obtained by GIMs at 12~14 LT, ±5º~±15º MLAT, 100º~150ºE every day in Asian sector are used to describe the variation in northern and southern EIA region, the results are shown in Figures 2c and 2d.

To demonstrate the dynamical process in EIA region, the EEJ is also used in this study, which can be estimated by the difference between the horizontal component of geomagnetic field at TIR (8.7°N, 77.8°E, MLAT~0.03°N) and VSK (17.68°N, 83.32°E, MLAT~8.56°N) (Rastogi et al., 1990). The results are shown in Figures 2e. In addition, the polar stratospheric temperature (90°S, 10hPa) and zonal mean zonal winds (60°S, 10hPa) obtained from National Centers for Environment Prediction (NCEP) are used to examine the extent of the SSW, the results are shown in Figures 2f and 2g. The background of geomagnetic activity index (Kp) and solar flux index (F10.7) from the websites http://spidr.ngdc.noaa.gov/ are depicted in Figures 2h and 2i.

3. Results and Analysis

It can be seen from Figures 2f and 2g that there were three obvious minor SH SSW events around day number 230-260 and a major SH SSW event around day number 263-288 (Olson et al., 2013). Figure 3 shows the contour map of polar stratospheric temperature (80°S, 10hPa) obtained from NCEP from July 20, 2002 to October 27, 2002. An eastward phase progression of quasi 10-day wave is clearly observed around day number 210-270. With SABER temperature data, Palo et al. (2005) also observed similar disturbance and suggested it consists of an eastward-propagating quasi 10-day wave with zonal wave numbers s=1

superimposed upon a large stationary planetary wave with s=1.

Now we examine the impact of this quasi 10-day wave on EIA region. 2002 was at solar maximum phase, the ionosphere maybe exhibit some variations caused by periodic solar irradiance and high speed solar streams related to solar rotation during 2002 SH SSW event, for example, 27-day periodic variation. To exclude these long period fluctuations in EIA region, the periods longer than 15 days in the MLAT location and TEC of EIA crest, and EEJ are removed. Specifically, these parameters are subtracted from their respective 15-day moving average. The residuals are subjected to Lomb-Scargle (L-S) spectral analysis (Lomb,1976; Scargle, 1982), and the results are shown in Figures 4a, 4b, 4c, 4d, and 4e. The horizontal dashed lines represent the 95% confidence level. It is evident that the MLAT location and TEC of EIA crest, and EEJ all exhibit significant quasi 10-day periodic component, which exceed or approach 95% confidence level, suggesting that the whole dynamical process in EIA region is modulated by quasi 10-day wave. Figures 4f and 4g show the L-S spectral analysis of Kp and F10.7. It can be seen that both Kp and F10.7 do not exhibit quasi 10-day periodic component, indicating that variation in the solar irradiance and geomagnetic activity cannot account for this quasi 10-day oscillation in EIA region.

To investigate the time evolution of quasi 10-day periodic variation, the Morlet wavelet spectral analysis is applied to MLAT location and TEC of EIA crest, EEJ and Kp. The periods longer than 15 days in the MLAT location and TEC of EIA crest , and EEJ are removed before the wavelet spectra is generated, and the results are illustrated in Figures 5a, 5b, 5c, 5d, and 5e. The black solid contours in each panel indicate a significance level higher than 95%. The white line in each panel represents the cone of influence of the wavelet analysis. The color bar number is the power strength for each parameter. Obviously, the most predominant periodic component in the MLAT location and TEC of EIA crest, and EEJ are quasi 10-day period, which mainly appeared around day number 210-290, indicating quasi 10-day oscillations in EIA region go through three minor SSWs and a major SSW period. The time evolution of the power in MLAT location and TEC of northern EIA crest match well those of southern EIA crest, respectively. In addition, we note both the MLAT location and the TEC of EIA crest show the quasi 2-day oscillations during major SSW period (around day number 260-270), which are also found on equatorial ionospheric electric fields and currents at the same period (Olson et al., 2013). Figure 5f shows the wavelet spectral analysis of Kp index. It can be seen that quasi 10-day periodic component is nearly absent in Kp around day number 230-290, suggesting that magnetic activity should not be the driving force for this quasi 10-day oscillation in EIA region.

In order to demonstrate the phase relationship of the quasi 10-day oscillations between northern and southern EIA crests, the band-pass filter is performed on the MLAT location and TEC of EIA crest. The absolute values of the MLAT location of EIA crest are used. The band-pass filter is centered at the period of 10-day, with half-power points at 8-day and 12-day, and the results are shown in Figure 6. The quasi 10-day wave amplitudes of northern and southern EIA crests are roughly equivalent, which exceed 1.7 degree for MLAT location and 7 TECU for TEC, respectively. Although the quasi 10-day wave of northern EIA crest match well those of southern EIA crest, the wave of northern EIA crest seemed to delay behind southern EIA crest, especially for MLAT location. To further verify this, Figure 7 shows the cross-correlation of quasi 10-day waves in MLAT location (a) and TEC (b) between northern and southern EIA crests. The cross-correlation coefficients of MLAT location and TEC reach 0.8 and 0.93, respectively. Moreover, the maximum cross-correlation coefficients for MLAT location is at 1 day, indicating that the wave of northern EIA crest delay 1 day behind southern EIA crest. This phase difference between northern and southern EIA crests may be due to differences in longitude between two GPS stations.

4. Discussions

In recent years a series of reports have focused on ionospheric perturbations during SSW event. The most predominant features in low latitude ionosphere associated with SSW event are semidiurnal pattern and 13- to 16-day periodic variations, which are attributed to nonlinear interaction of planetary wave, solar and lunar tide wave (Pedatella and Forbes, 2009;Goncharenko et al., 2010; Fejer et al., 2010;Park et al., 2012). As major SSW often occurs in NH, most studies about SSW effects on the ionosphere are during NH SSW period. In August to September 2002, the first major SSW was observed in SH. The NH and SH SSW occurred in Arctic and Antarctic winter, respectively, so the occurring time and location of SH SSW are opposite to those of NH SSW. The researches of ionospheric behavior during SH SSW periods are useful for testing the general rule of ionospheric perturbations during NH SSW periods. For example, Olson et al. (2013) demonstrated that multi-day ionospheric perturbations responding to 2002 SH SSW resemble those observed during NH SSWs and these ionospheric perturbations were associated with enhanced lunar tidal effects.

In this study we present observations of quasi 10-day oscillation in EIA region during the 2002 SH SSW that has not been reported during NH SSWs. This quasi 10-day periodic component is absent or very weak in Kp and F10.7 index, indicating that the magnetic activity and solar irradiance cannot account for

this quasi 10-day oscillation in EIA region. Meanwhile, an unusual atmospheric state occurred in this period that the ozone hole over the Antarctic has a smaller size and splits into two separate holes (Varotsos 2002; Baldwin et al., 2003). This phenomenon is thought to be due to high temperatures in the Antarctic stratosphere, which was contributed to by upward propagation of planetary waves (Venkat Ratnam et al., 2004). Moreover, strong planetary wave scale quasi 10-day variation was observed in polar stratospheric temperature during this period. The wave interactions between eastward-propagating waves with periods near 10 days, quasi-stationary planetary waves, and the zonal mean atmospheric state were eventually driven towards total break-down of the polar vortex and a major warming of the stratosphere (Krüger et al., 2005; Palo et al., 2005). So the quasi 10-day oscillations in EIA region should be ascribed to atmosphere perturbations linking the SSW in the Southern Hemisphere.

The coupling process of 10-day oscillation between the lower atmosphere and ionosphere can be demonstrated by existing observations and simulations. A series of studies have showed how the quasi 10-day planetary wave in stratosphere can penetrate into the ionosphere E region (Krüger et al., 2005; Palo et al., 2005; Chang et al., 2009). Krüger et al. (2005) revealed the eastward-traveling waves with periods near 10 days and their interaction with quasi-stationary planetary waves forced in the troposphere during 2002 SH SSW event, supporting the observational and numerical evidence that the eastward traveling wave interacts with the stationary wave to produce a quasi-periodic amplitude modulation of the stationary waves (Hirota et al., 1990; Ushimaru and Tanaka, 1992). Palo et al. (2005) found an eastward-propagating quasi 10-day wave with zonal wave numbers s=1 and s=2, and a quasi-stationary planetary waves with s=1 extend from the lower stratosphere to the 100-120 km height region with little amplitude attenuation. While the quasi-stationary planetary wave is confined to the high latitude atmosphere and cannot directly propagate to equatorial ionosphere, the tides were introduced into planetary wave modulation mechanism. Eswaraiah et al. (2018) reported that zonal diurnal and semidiurnal tide amplitudes in Antarctica mesosphere and lower thermosphere were enhanced around day number 230-290 during 2002 SH SSW, which coincides with the enhanced period of quasi 10-day oscillations in EIA region shown in Figure 5. Moreover, Chang et al. (2009) showed that the short-term variability of the s=1 semidiurnal tide is strongly dependent upon the PW1 events (quasi-10-day wave) prior to the major warming during 2002 SH SSW, supporting the suggestion that the quasi-stationary planetary wave can influence migrating and nonmigrating solar tides globally (Liu et al., 2010; Pedatella and Forbes, 2010). So the interactions between quasi-10-day planetary wave and tide will modify the ionosphere E-region winds, which can produce

E-region electric fields via the E-region dynamo process. In this study, the EEJ driven by equatorial zonal electric field also exhibits quasi 10-day oscillation, indicating that the upward-propagating planetary waves interacted with the tide produced oscillation in EIA region through modulating E-region electric fields. Specifically, the E-region electric fields map to lower ionospheric F-region along the magnetic field lines and generate an eastward electric field (Goncharenko et al., 2010). At the magnetic equator, the eastward electric field with quasi 10-day periodic variation change electron density distribution in the low-latitude region via E×B drift, and finally leads to quasi 10-day planetary waves characteristic variations in EIA region. Previous studies have revealed a strong correlation between ionospheric perturbations and the occurrence of NH SSW. During NH SSW period, quasi 16-day oscillations and semidiurnal pattern are observed in equatorial mesopause temperature, the MLT meridional and zonal wind, EEJ, electron density and TEC (Vineeth et al., 2007; Pedatella and Forbes, 2009; Park et al., 2012 ; Jonah et al., 2014). Some researchers attribute these ionospheric perturbations to the strong dynamical coupling between the lower atmosphere and ionosphere through the intensification of planetary wave activity (Chau et al., 2009), lunar (Fejer et al., 2010) and solar (Pedatella et al., 2012) tide. In this study, the consistent quasi 10-day oscillations appear in EEJ, the location and TEC of northern and southern EIA crest, indicating that coupling mechanism between the lower atmosphere and ionosphere during SH SSW period is consistent with that during NH SSW period.

In our prior studies, a 14- to 15-day wave during several NH SSW events is ascribed to lunar tide (Mo et al., 2018). So the source of quasi 10-day oscillations in EIA region during 2002 SH SSW is different from 14- to 15-day waves during NH SSW. For this 10-day periodic event, it seems that the effect of the planetary wave is more obvious. Moreover, no obvious 14- to 15-day oscillation is found in EIA region during 2002 SH SSW, which may be that the equatorial lunar semidiurnal effects during September-October are weaker than that during January-February (Stening et al., 2011; Pedatella, 2014). Olson et al. (2013) also reported that the perturbations amplitude of EEJ and vertical drifts modulated by lunar semidiurnal tides during SH SSW are smaller than those during NH SSW.

5. Conclusions

Using the location and TEC of EIA crests derived from GPS station observations and GIMs, we found a quasi 10-day periodic variability in northern and southern EIA region in Asian sector during the SH SSW of 2002. In the same time period, this quasi 10-day oscillation is also seen in the polar stratospheric

241 temperature, which is absent and weak in Kp and F10.7 index, respectively. The SH SSW of 2002 itself is
242 generated by quasi 10-day planetary wave. Previous studies have shown that a strong quasi 10-day
243 planetary wave with zonal wave numbers s=1 extend from the lower stratosphere to mesosphere and lower
244 thermosphere during the SH SSW of 2002 (Palo et al., 2005). Moreover, the EEJ driven by equatorial zonal
245 electric field exhibits quasi 10-day oscillation, indicating that the upward-progagating planetary waves
246 interacted with the tide will modify E-region electric fields, thereby altering the plasma structures through
247 upward E×B drift, which results in the periodical variations in these ionospheric parameters in F region.
248 These results support the suggestion that the quasi 10-day variation in EIA region should be ascribed to
249 enhanced 10-day planetary wave in lower atmosphere associated with SSW.

250 **Acknowledgements:** The GPS data were from the Crustal Movement Observation Network of China (via
251 e-mail to yglyang@cma.gov. cn) and IGS (available at http://sopac. ucsd.edu). The geomagnetic data at
252 TIR and VSK were from WDC for Geomagnetism, Kyoto (available
253 at http://wdc.kugi.kyoto-u.ac.jp/hyplt/index.html). The GIMs were downloaded from the site
254 ftp://cddis.gsfc.nasa.gov. This research was jointly supported by the National Natural Science Foundation
255 of China (41864006, 41674157, and 41464006), Guangxi Natural Science Foundation
256 (2016GXNSFAA380132), and Chinese Meridian Project. We gratefully acknowledge National Center for
257 Environmental Prediction (NCEP) for providing public access to stratospheric data (available at
258 https://www. esrl.noaa.gov/psd/data/reanalysis/).

259 **References**

260 Andrews, D. G., Holton, J. R., and Leovy, C. B.: Middle Atmosphere Dynamics, Academic, San Diego,
261 Calif, 1987.
262 Andrew, J. D., Vincent, R. A., Murphy, D. J., Tsutsumi, M., Riggin, D. M., and Jarvis, M. J.: The
263 large-scale dynamics of the mesosphere-lower thermosphere during the Southern Hemisphere
264 stratospheric warming of 2002, Geophys. Res. Lett, 31, L14102, doi:10.1029/2004GL020282, 2004
265 Baldwin, M., Hirooka, T., O'Neill, A., and Yoden, S.: major stratospheric warming in the Southern
266 Hemisphere in 2002: Dynamical aspects of the ozone hole split, SPARC Newsl., 20, 24-26, 2003.
267 Chang, L. C., Palo, S. E., and Liu, H. -L.: Short-term variation of the s=1 nonmigrating semidiurnal tide
268 during the 2002 stratospheric sudden warming, J. Geophys. Res., 114, D03109,
269 doi:10.1029/2008JD010886, 2009.
270 Chau, J. L., Fejer, B. G., and Goncharenko, L. P.: Quiet variability of equatorial E × B drift during a

sudden stratospheric warming event. Geophys. Res. Lett, 36, L05101, https://doi.org/10.1029/2008GL036785, 2009.

Eswaraiah, S., Kim, Y. H., Lee, J., Ratnam, M. V., and Rao, S. V. B.: Effect of Southern Hemisphere sudden stratospheric warmings on Antarctica mesospheric tides: First observational study. J. Geophys. Res. Space Physics, 123, 2127–2140, https:// doi.org/10.1002/2017JA024839, 2018.

Fejer, B. G., Olson, M. E., Chau, J. L., Stolle, C., Lühr, H., Goncharenko, L. P., Yumoto, K., and Nagatsuma, T.: Lunar-dependent equatorial ionospheric electrodynamic effects during sudden stratospheric warmings, J. Geophys. Res., 115, A00G03, doi:10.1029/2010JA015273, 2010.

Goncharenko L. P., Chau, J. L., Liu, H. -L., and Coster, A. J.: Unexpected connections between the stratosphere and ionosphere, Geophys. Res. Lett., 37, L10101, doi:10.1029/2010GL043125, 2010.

Hirota, I., Kuroi, K., and Shiotani, M.: Midwinter warmings in the Southern Hemisphere stratosphere in 1988, Q. J. R. Meteorol., Soc., 116, 929-941, 1990.

Hofmann‐Wellenhof, B., Lichtenegger, H., and Collins, J.: GPS—Theory and Practice, Springer, New York, 1992.

Huang, Y. N., Cheng, K., and Chen, S. W.: On the equatorial anomaly of the ionospheric total electron content near the northern anomaly crest region, J. Geophys. Res., 94(A10), 13,515–13,525, 1989.

Jin, H., Miyoshi, Y., Pancheva, D., Mukhtarov, P., Fujiwara, H., and Shinagawa, H.: Response of the migrating tides to the stratospheric sudden warming in 2009 and their effects on the ionosphere studied by a whole atmosphere-ionosphere model GAIA with COSMIC and TIMED/SABER observations, J. Geophys. Res., 117, A10323, doi:10.1029/2012JA017650, 2012.

Jonah, O. F., de Paula E. R., Kherani, E. A., Dutra, S. L. G., and Paes, R. R.: Atmospheric and ionospheric response to sudden stratospheric warming of January 2013, J. Geophys. Res. Space Physics, 119, 4973–4980, doi.org/10.1002/2013JA019491, 2014.

Krüger, K., Naujokat, B., and Labitzke, K.: The unusual midwinter warming in the Southern Hemisphere stratosphere 2002: A comparison to Northern Hemisphere phenomena, J. Atmos. Sci., 62, 603-613, 2005.

Liu, H. -L, Wang, W., Richmond, A. D., and Roble, R. G.: Ionospheric variability due to planetary waves and tides for solar minimum conditions, J. Geophys. Res., 115, A00G01, doi:10.1029/2009JA015188, 2010.

Lomb, N. R.: Least-squares frequency analysis of unequally spaced date, Astrophys.Space Sci., 39,

447-462, 1976.

Mannucci, A. J., Wilson, B. D., Yuan, D. N., Ho, C. M., Lindqwister, U. J., and Runge, T. F.: A global mapping technique for GPS derived ionospheric total electron content measurements, Radio Sci., 33, 565-582, doi:10.1029/97RS02707, 1998.

Matsuno, T.: A dynamical model of the stratospheric sudden warming, J. Atmos. Sci., 28, 1479-1494, 1971.

Mo, X. H., Zhang, D. H., Goncharenko, L. R., Hao, Y. Q., and Xiao, Z.: Quasi-16-day periodic meridional movement of the equatorial ionization anomaly, Ann. Geophys., 32, 121-131, 2014.

Mo, X. H., Zhang, D. H., Goncharenko, L. R., Zhang, S. R., Hao, Y. Q., Xiao, Z., Pei, J. Z., Yoshikawa, A., Chau, H. D.: Meridional movement of northern and southern equatorial ionization anomaly crests in the East-Asian sector during 2002–2003 SSW, Science China Earth Sciences, 60(4), 776–785, https://doi.org/10.1007/s11430-016-0096-y, 2017.

Mo, X. H., and Zhang, D. H.: Lunar tidal modulation of periodic meridional movement of equatorial ionization anomaly crest during sudden stratospheric warmaing, J. Geophys. Res. Space Physics, 123, 1488-1499. https://doi.org/10.1002/2017JA024718, 2018.

Olson, M. E., Fejer, B. G., Stolle, C., Lühr, H., and Chau, J. L.: Equatorial ionospheric electrodynamic perturbations during Southern Hemisphere stratospheric warming events, J. Geophys. Res. Space Physics, 118, 1190-1195, doi:10.1002/jgra.50142, 2013.

Palo, S. E, Forbes, J. M., Zhang, X., Russell III, J. M., Mertens, C. J., Mlynczak, M. G., Burns, G. B., Espy, P. J., and Kawahara, T. D.: Planetary wave coupling from the stratosphere to the thermosphere during the 2002 Southern Hemisphere pre-stratwarn period, Geophys. Res. Lett., 32, L23809, doi:10.1029/2005GL024298, 2005.

Pancheva, D, and Mukhtarov, P.: Stratospheric warmings: The atmosphere-ionosphere coupling paradigm, J. Atmos. Sol. Terr. Phys., 73, 1697-1702, doi:10.1016/j.jastp.2011.03.006, 2011.

Park, J., Lühr, H., Kunze, M., Fejer, B. G., and Min, K. W.: Effect of sudden stratospheric warming on lunar tidal modulation of the equatorial electrojet, J. Geophys. Res., 117, A03306, doi:10.1029/2011JA017351, 2012.

Pedatella, N. M., and Forbes, J. M.: Modulation of the equatorial F-region by the quasi-16 day planetary wave, Geophys. Res. Lett., 34, L09105, doi:10.1029/2009GL037809, 2009.

Pedatella, N. M., and Forbes, J. M.: Evidence for stratosphere sudden warming-ionosphere coupling due to vertically propagating tides, Geophys. Res. Lett., 37, L11104, doi:10.1029/2010GL043560, 2010.

Pedatella, N. M., Liu, H. L., and Richmond, A. D.: Atmospheric semidiurnal lunar tide climatology simulated by the Whole Atmosphere Community Climate Model, J. Geophys. Res., 117, A06327, doi:10.1029/2012JA017792, 2012.

Pedatella, N. M.: Observations and simulations of the ionospheric lunar tide: Seasonal variability, J. Geophys. Res. Space Physics, 119, 5800-5806, doi:10.1002/2014JA020189, 2014.

Rastogi, R. G., and Klobuchar, J. A. : Ionospheric electron content within the equatorial F2 layer anomaly belt, J. Geophys. Res., 95(A11), 19,045–19,052, https://doi.org/10.1029/JA095iA11p19045, 1990.

Scargle, J. D.: Studies in astronomical time series analysis. II. Statistical aspects of spectral analysis of unevenly spaced data, Astrophys. J., 263, 835-853, 1982.

Scherhag, R.: Die explosionsartigen Stratosphärenerwärmungen des Spätwinters 1952, Ber. Dtsch Wetterdienstes USZone, 6, 51-63, 1952.

Stening, R. J.: Lunar tide in the equatorial electrojet in relation to stratospheric warmings, J. Geophys. Res., 116, A12315, doi:10.1029/2011JA017047, 2011.

Ushimaru, S., and Tanaka, H.: A numerical study of the interaction between stationary Rossby waves and eastward-traveling waves in the Southern Hemisphere stratosphere, J. Atmos., Sci., 49, 1354-1373, 1992.

Varotsos, C.: The Southern Hemisphere ozone hole split in 2002, Environ. Sci. Pollut. Res., 9, 375-376, 2002.

Venkat Ratnam, M., Tsuda, T., Jacobi, C., and Aoyama, Y.: Enhancement of gravity wave activity observed during a major Southern Hemisphere stratospheric warming by CHAMP/GPS measurements, Geophys. Res. Lett., 31, L16101, doi:10.1029/2004GL019789, 2004.

Vineeth, C., Pant, T. K., Devasia, C. V., and Sridharan, R.: Atmosphere-ionosphere coupling observed over the dip equatorial MLTI region through the quasi 16-day wave. Geophys. Res. Lett., 34, L12102, https://doi.org/10.1029/2007GL030010, 2007.

Yeh, K. C., Franke, S. J., Andreeva, E. S., and Kunitsyn, V. E.: An investigation of motions of the equatorial anomaly crest, Geophys. Res. Lett., 28(24), 4517-4520, doi:10.1029/2001GL013897, 2001.

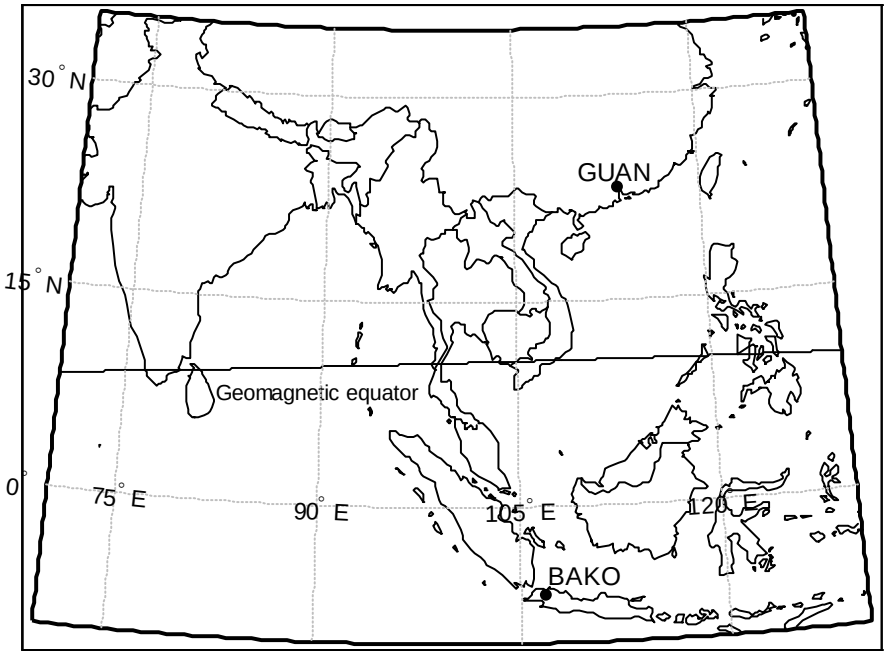

Figure 1. Location of the GPS stations in Asian sector.

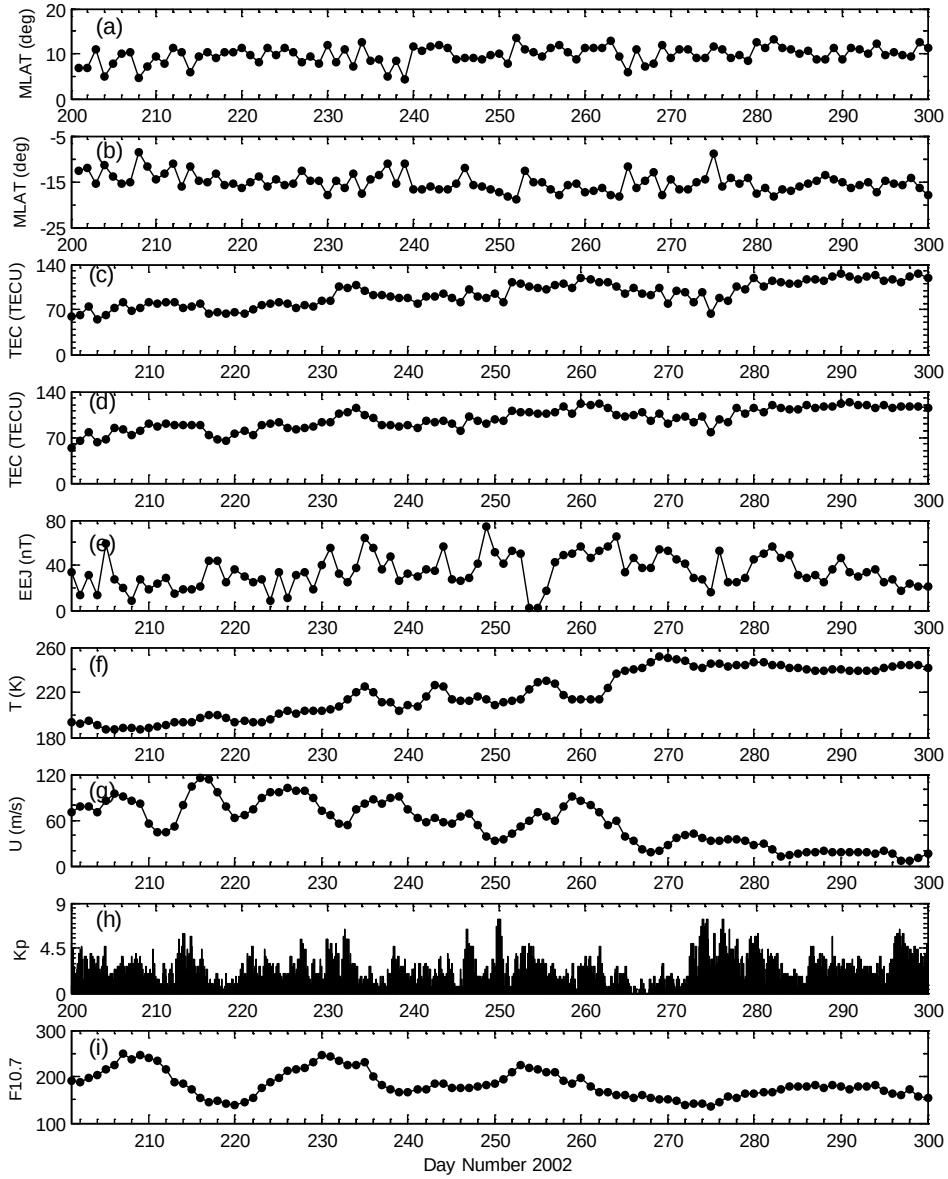

363

364 **Figure 2.** The magnetic latitude (MLAT) location of (a) northern and (b) southern equatorial ionization
365 anomaly (EIA) crest; The TEC of (c) northern and (d) southern EIA crest; the (e) equatorial electrojet (EEJ),
366 (f) polar stratospheric temperature (at 90°S, 10hPa) and (g) zonal wind (at 60°S, 10hPa) from National
367 Centers for Environment Prediction; the (h) Geomagnetic activity index, Kp and (i) solar flux index F10.7
368 during the period from July 20, 2002 to October 27, 2002.

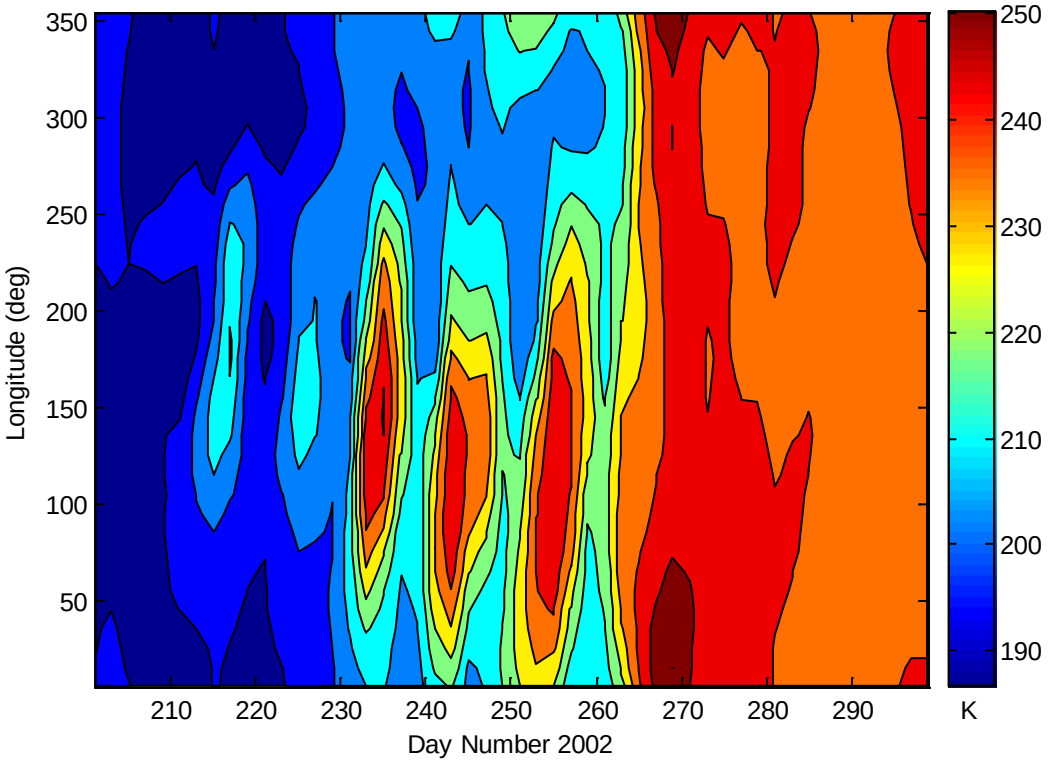

Figure 3. The contour map of polar stratospheric temperature (80°S, 10hPa) obtained from NCEP during the same period as in Figure 2.

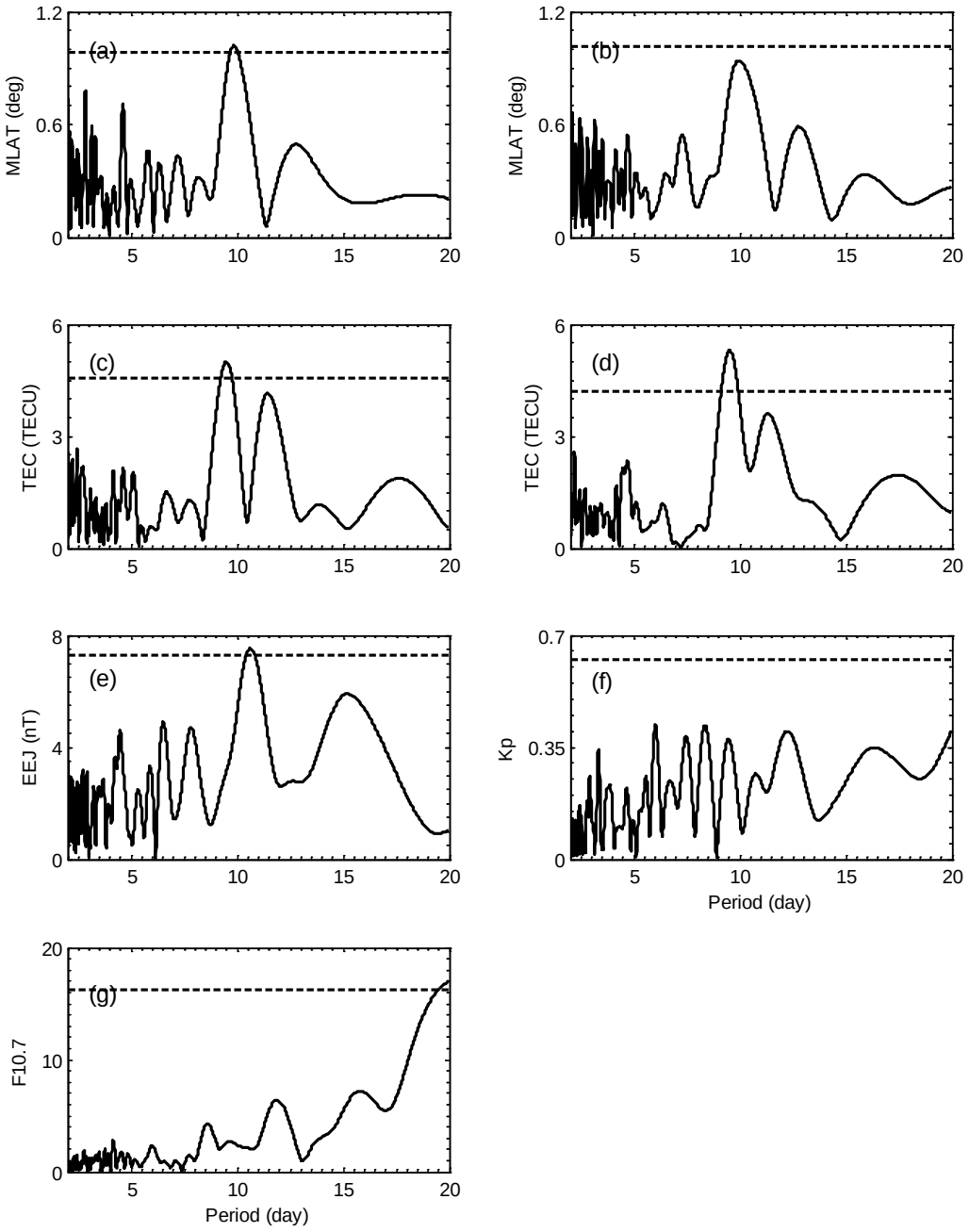

372

373 **Figure 4.** Lomb-Scargle periodgrams of the MLAT location of (a) northern and (b) southern EIA crest, the
374 TEC of (c) northern and (d) southern EIA crest, (e) EEJ, (f) Kp index and (g) F10.7 during the same period
375 as in Figure 2.

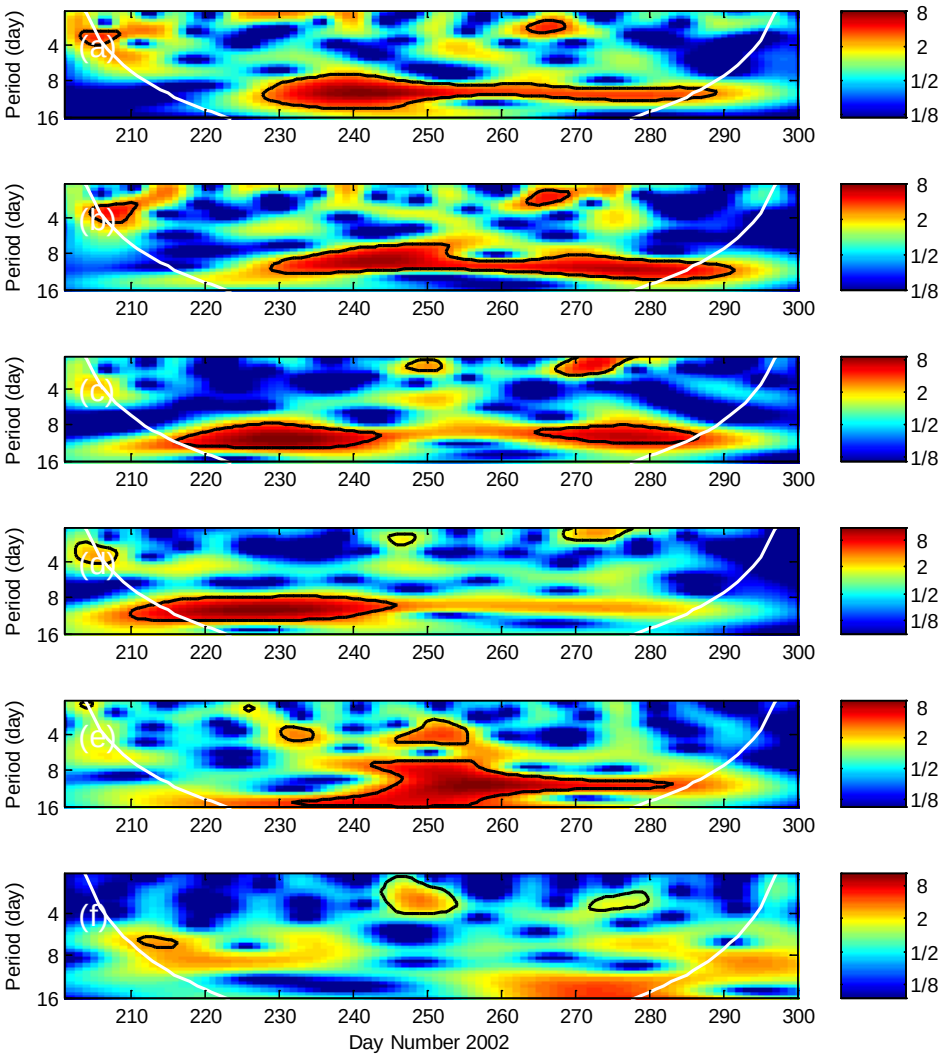

376

377 **Figure 5.** The wavelet power spectra of the MLAT location of (a) northern and (b) southern EIA crest, the

378 TEC of (c) northern and (d) southern EIA crest, (e) EEJ and (f) Kp index during the same period as in

379 Figure 2. The white line in each panel represents the cone of influence of the wavelet analysis.

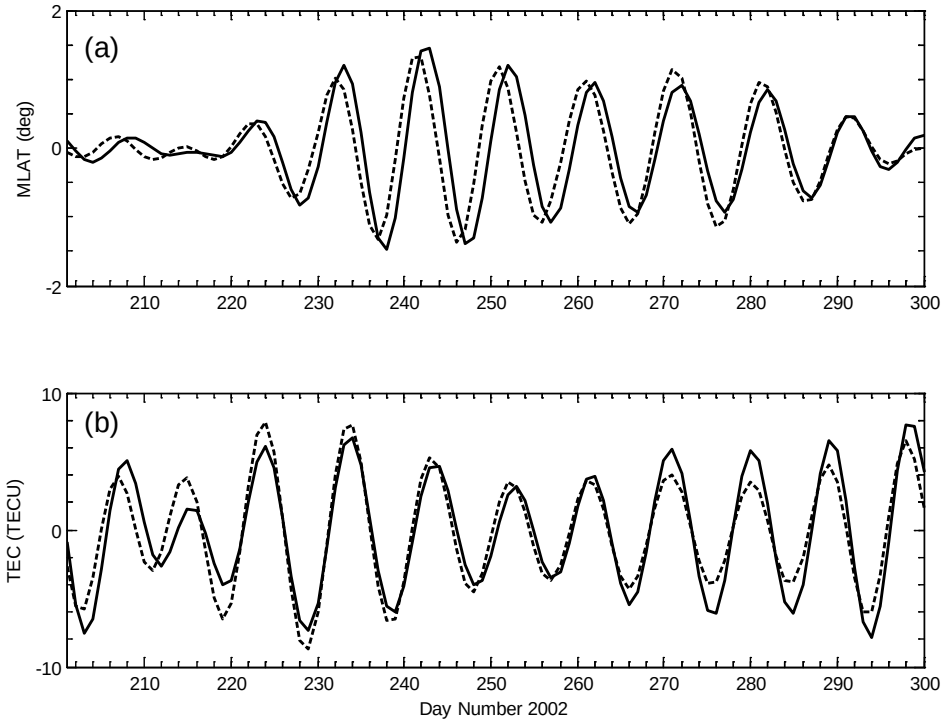

380

381 **Figure 6.** The band-pass filter results of the (a) MLAT location of (solid line) northern and (dash-dotted

382 line) southern EIA crest, the (b) TEC of (solid line) northern and (dash-dotted line) southern EIA crest

383 during the same period as in Figure 2.

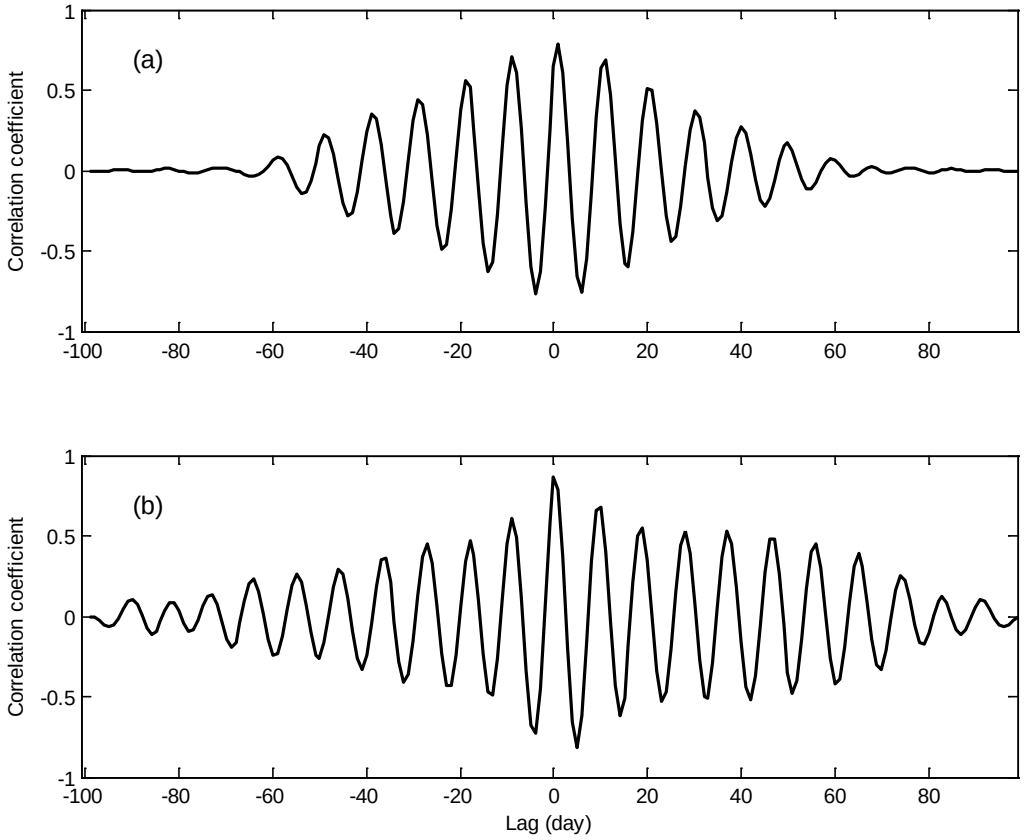

384

385 **Figure 7.** The cross-correlation of quasi 10-day waves in MLAT location (a) and TEC (b) between northern

386 and southern EIA crest.